Accurate Visible Light Positioning Using Multiple-Photodiode Receiver and Machine Learning

Adli Hasan Abu Bakar, Tyrel Glass, Hing Yan Tee, Fakhrul Alam, *Senior Member, IEEE,* and Mathew Legg, *Member, IEEE*

***Abstract*— Visible light positioning (VLP) is a promising indoor localization method as it provides high positioning accuracy and allows for leveraging the existing lighting infrastructure. Photodiode (PD)-based receiver is a commonly used tag for VLP. However, a tag employing a single PD requires three or more luminaires to be visible. This article presents a VLP system that uses a custom-made tag utilizing multiple PDs. It applies received signal strength (RSS)-based fingerprinting using a weighted k-nearest neighbor (WkNN) algorithm for localization. Experimental results show that it is possible to localize using less than three luminaires with high accuracy. The Manhattan and Matusita distance metrics are found to provide lower localization accuracy than the Euclidean metric for the WkNN algorithm. The creation of a dense fingerprinting database through 2-D interpolation is presented as a method to reduce the cost of time and labor. The localization performance of the VLP system does not degrade noticeably with the fabricated database. The localization accuracy of the WkNN algorithm is shown to be better than that of a multilayer perceptron (MLP)-based regressor. The developed VLP system is also experimentally benchmarked against the HTC Vive showing comparable performance.**

***Index Terms*— Artificial neural network (ANN), indoor localization, indoor positioning system (IPS), machine learning (ML), multilayer perceptron (MLP), visible light positioning (VLP), weighted k-nearest neighbors (WkNNs).**

I. Introduction

GLOBAL positioning system (GPS) has been used in many applications, such as localization, navigation, tracking, mapping, and timing. Although GPS can be used to locate a target outdoors, it is very difficult to do so if the target is located indoors due to the inability of GPS signals to penetrate through walls [1]. Accurate positioning of a person or an object indoors can facilitate many applications, such as navigation in large indoor environments such as airports or shopping malls [2]. Multiple technologies have been proposed for indoor localization, such as wireless [3], visible light [4], and ultrasound [5], to name a few. Wireless-based technologies are vulnerable to multipath and interference [6], while ultrasound comes with high installation costs [7]. Recently, visible light positioning (VLP) has garnered the interest of researchers due to the convenience of implementation using light-emitting diode (LED) luminaires. Visible light signals do not pass through walls making them secure [8], and visible light-based positioning systems can potentially offer higher accuracy compared with other technologies [9].

Visible light characteristics that are commonly used for VLP are received signal strength (RSS), time of arrival (TOA) [10], Time Difference of Arrival (TDoA) [11], and Angle of Arrival (AoA) [12]. RSS-based systems may produce low accuracy due to sensitivity and tilt issues [13], while AoA-based systems may provide comparatively higher accuracy but are more complex [14]. TDoA-based systems can also achieve high localization accuracy [11] but are complex and costly to implement as they require synchronization between hardware [15]. Therefore, the most popular VLP techniques use RSS [16]. RSS values obtained from a light sensor, e.g., a photodiode (PD), can be used to determine the distance between the transmitter (i.e., the luminaire) and receiver/tag [17]. Based on this ranging, techniques such as trilateration [18] can be applied for localization. RSS from multiple luminaires can also be used as features for fingerprinting-based localization [19].

A. Multiple Photodiode Systems

A single-PD-based VLP system requires at least three luminaires for effective localization. However, that many luminaires may not be visible to the PD in some real-world environments. To overcome this problem, multiple-PD-based VLP systems that can function with less than three luminaires within the PDs' field of view (FOV) have been proposed [20]–[23]. Multiple-PD receivers can also be used to mitigate the tilt issue [24] of single-PD receivers. The reported VLP systems in the literature use three [11], [20], [22], [23], [25] or more [4], [9], [26], [27] PDs.

The difference in angles and position of a multi PD receiver design can be exploited to develop novel localization methods. For example, RSS from multiple PDs, RSS ratio [23], [26],

Manuscript received June 22, 2020; revised August 21, 2020; accepted September 10, 2020. Date of publication September 21, 2020; date of current version December 4, 2020. The work of Adli Hasan Abu Bakar and Tyrel Glass was supported in part by the Massey University Doctoral Scholarships. The Associate Editor coordinating the review process was Lihui Peng. *(Corresponding author: Fakhrul Alam.)*

The authors are with the Department of Mechanical and Electrical Engineering (MEE), School of Food & Advanced Technology (SF&AT), Massey University, 0632 Auckland, New Zealand (e-mail: a.hasan@massey.ac.nz; t.glass@massey.ac.nz; hingyantee@gmail.com; f.alam@massey.ac.nz; m.legg@massey.ac.nz).

Digital Object Identifier 10.1109/TIM.2020.3024526

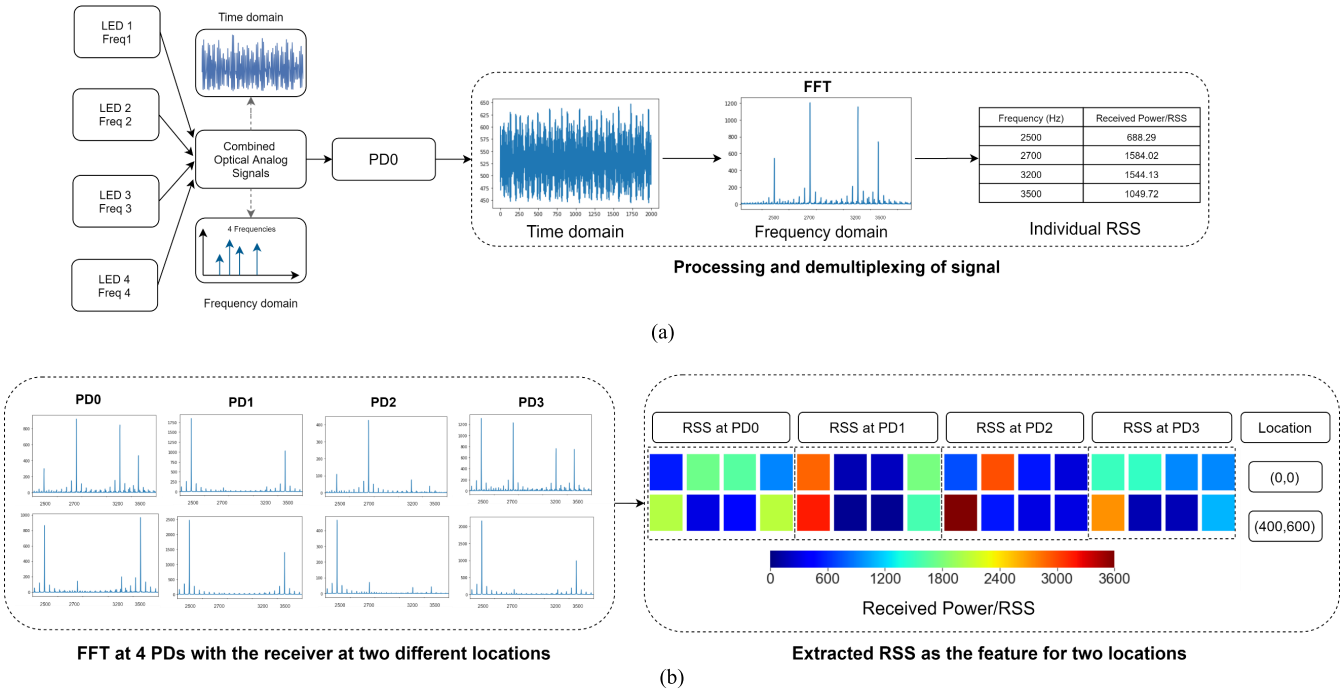

Fig. 1. Key concept of the proposed VLP system. (a) Extraction of RSS from one PD. This is performed for all four PDs. (b) Extracted RSS from the four PDs can be considered a distinct feature for a location. Examples of two separate locations shown.

[27], and RSS difference [22] between the PDs can be used to estimate the position of the receiver. Xie *et al.* [4] used the linear independence of the multiple-PD planes, while Yasir *et al.* [9] utilized the RSS and incidence angle. It should be noted that single-PD systems that use a rotating receiver [21], [28], [29] can also emulate multiple-PD-based systems. Researchers have proposed a VLP system using a rotatable single-PD receiver where the receiver takes the RSS at a single location at different angles [24]. The authors further developed this system by using the same positioning method but using a receiver with three tilted PDs instead [25]. Table I summarizes the reported works on multiple-PD systems available in the literature. As can be observed, all implementations of the reported multiple-PD-based VLP systems utilize modeling, and there is a lack of literature on machine learning (ML)-based multiple-PD systems. Therefore, in this work, we are exploring a multiple-PD-based system that applies ML techniques for localization.

B. Machine Learning for Localization

ML techniques have been widely investigated for wireless-based indoor positioning [30]–[32]. However, it has not been well utilized for VLP. While ML techniques, such as WkNN [33] and artificial neural network (ANN) [34], have been reported for VLP, they have not been utilized for multiple-PD-based VLP systems.

Creating a fingerprint with an off-line database is a key step of ML-based localization. Such localization methods consist of two phases: offline and online [35]. In the off-line phase, fingerprints or features of an environment are collected at the target device (e.g., RSS) and are stored in a database. In the online phase, the data obtained from the target in real-time are then compared with the values stored in the database, and the position of the device is estimated.

The research presented here extends the work reported in [36] and offers the following original contributions.

1) *Accurate VLP System Using Multiple PDs and ML:* This is the first reported work that implements a multiple-PD-based VLP system employing fingerprinting and ML algorithms for accurate localization. In contrast to single-PD-based systems, the developed VLP system can localize accurately when only two luminaires are visible. Experimental results show that there is only minimal degradation in localization accuracy when going from four luminaires to two.
2) *Impact of Distance Metric on the Localization Accuracy of the Weighted K-Nearest Neighbor (WKNN) Regressor:* Two distance metrics, Manhattan and Matusita, outperformed the common Euclidean metric in terms of localization accuracy.
3) *Reduced Fingerprinting Cost Through Data Fabrication:* Fingerprinting incurs a significant cost of time and labor for off-line site surveying. Data fabrication through 2-D interpolation is shown to be an effective way of constructing a dense fingerprint database from a sparse one and thus reducing the cost of fingerprinting.
4) *Comparison Between WkNN and Multilayer Perceptron (MLP), Two ML Algorithms, With Respect to Localization Accuracy:* Experimental results show that, for the setup utilized, WkNN outperforms MLP.
5) *Benchmarking Against Commercial Tracking Solution:* Unfortunately, VLP systems reported in the literature have not been experimentally benchmarked against existing commercial products and are only compared with other proposed techniques. In contrast,

TABLE I
OVERVIEW OF WORKS ON MULTIPLE-PD VLP SYSTEMS

Research	Localization Error (mm)	Method	Machine Learning	Number of PDs	Number of luminaires	Limitations
Xie, et.al [4]	Mean ≈ 400.0	Channel model-based RSS	No	6	1	-Transmitter and receiver need to be parallel -Low accuracy
Yasir, et.al [9]	Mean ≈ 60.0		No	4	3	-Positioning algorithm complexity
Yu, et.al [26]	Mean ≈ 34.0		No	4	1	-Simulation only; no hardware implementation -Transmitter and receiver need to be parallel
Yang, et.al [20]	Mean ≈ 65.0		No	3	1	
Xu, et.al [22]	Mean ≈ 40.0		No	2	2	
Yu, et.al [23]	Mean ≈ 21.5		No	3	1	
Yang, et.al [25]	Mean ≈ 30.0	RSS difference-based fingerprinting	No	3	1	-Simulation only; no hardware implementation -Requires predefined RSS difference as database
Naz, et.al [11]	Mean ≈ 0.13	TDoA	No	4	1	-Simulation only; no hardware implementation -Hardware needs be synchronized
Wang, et.al [27]	90^{th} percentile ≈ 100	AoA based on channel model	No	4	4	-Simulation only; no hardware implementation -Low accuracy
Proposed	90^{th} percentile ≈ 12.12 Median ≈ 4.74	RSS-based fingerprinting with fabricated data	Yes	4	4	-Requires fingerprint database -Receiver orientation needs to stay unchanged
	90^{th} percentile ≈ 48.77 Median ≈ 9.87		Yes	4	2	

the performance of the developed VLP system is benchmarked against a consumer product HTC Vive. The localization accuracy of the proposed system is found to be similar to that of the Vive.

The rest of this article is organized as follows. Section II describes the hardware of the developed VLP system, the data acquisition system, and the experimental setup. Section III introduces the WkNN algorithm as a classifier for the VLP system. Section IV discusses experimental results and findings for the WkNN algorithm. It presents an ANN-based localization algorithm and compares its positioning accuracy with that of WkNN. Section V demonstrates how data fabrication can reduce the cost of an off-line site survey. Section VI benchmarks the localization performance of the proposed system against the HTC Vive. Section VII concludes this article with suggestions for future work.

II. SYSTEM OVERVIEW

The developed VLP system is based on frequency-division multiplexing (FDM) with the demultiplexing done at the receiver through a fast Fourier transform (FFT). Fig. 1 shows a block diagram of the process where each of the four LED luminaires transmits a discrete tone. At the multiple-PD receiver board, the sum of the discrete tones is received, and demultiplexing is performed to separate the discrete tones for each luminaire. The FFT of the output of the PD-based light sensors is computed, and the received power at each unique frequency is used as a measure of RSS for the corresponding luminaire. As can be observed, the RSS can be a distinctive feature for a location.

A. Transmitter

Custom modulation boards were used to drive four consumer-grade LED luminaires so that each luminaire is able to transmit unmodulated sine waves at frequencies between 2 and 4 kHz [37]. For the experiments conducted, the luminaires are set to unique frequencies of 2.5, 2.7, 3.2, and 3.5 kHz, respectively.

B. Receiver

To receive the optical signals from the luminaires, a custom-made receiver board using an ESP8266 microcontroller was designed. The design of the receiver board is a triangular base with three PDs tilted at an angle of 60° and a single horizontal PD located in the middle, as shown in Fig. 2.

A two-stage op-amp circuit was designed to capture the discrete tone signals from the luminaires through the reverse bias current of a PD. The current is then converted into a voltage signal and is read by an ADC, which has a sampling rate of 20 kHz. The op-amp circuit is also able to filter out the low-frequency (e.g., 100-Hz powerline flicker) and steady-state dc signals generated by ambient light. The lower corner and upper corner frequencies of the op-amp are designed to be 550 and 4800 Hz, respectively. The receiver board also includes an inertial measurement unit (IMU) to measure the orientation of the receiver if needed.

C. Data Collection and Experimental Setup

The vertical distance between the receiver board and the luminaires is 1600 mm. A 2-D CNC machine with dimensions of 1200 × 1200 mm was utilized for taking measurements. The position of the CNC machine is controlled by providing the *XY* coordinate of the desired location. The CNC machine has an accuracy of 0.025 mm, making it orders of magnitude better than the expected localization accuracy of the developed system. Therefore, it is appropriate for recording the ground truth and RSS data in an accurate and automated manner. The custom-made receiver board was mounted onto the CNC machine to ensure that its orientation is kept constant throughout the experiment. Fig. 3 shows the experimental setup with the luminaires, CNC machine, and receiver board.

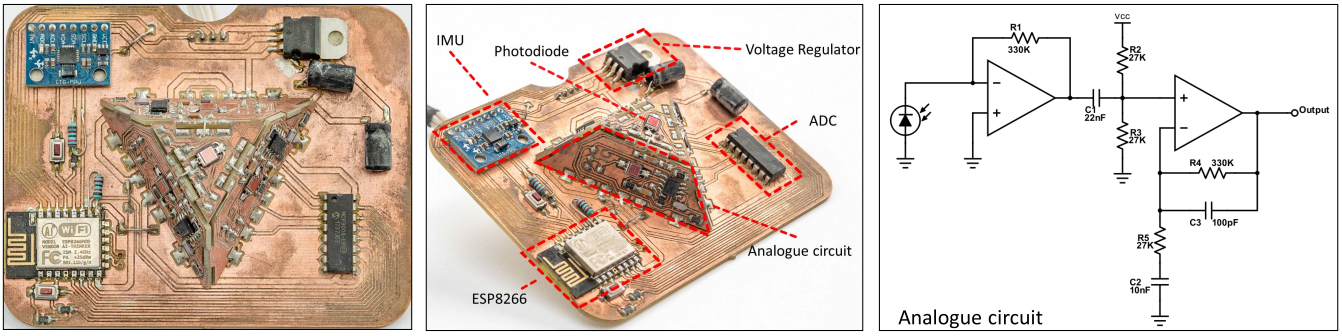

Fig. 2. Details of the custom-designed multiphotodiode receiver board.

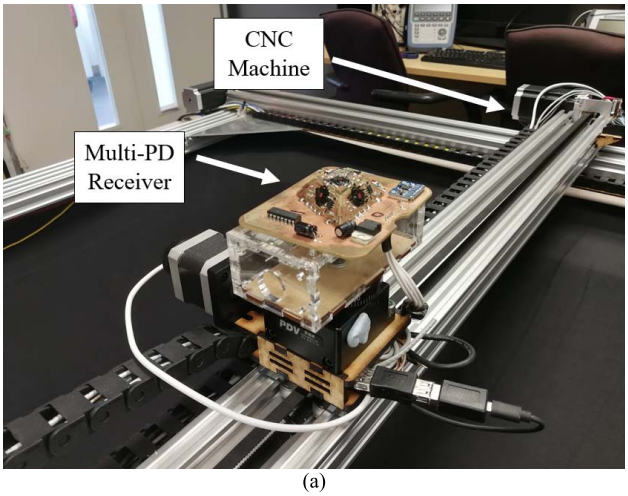

(a)

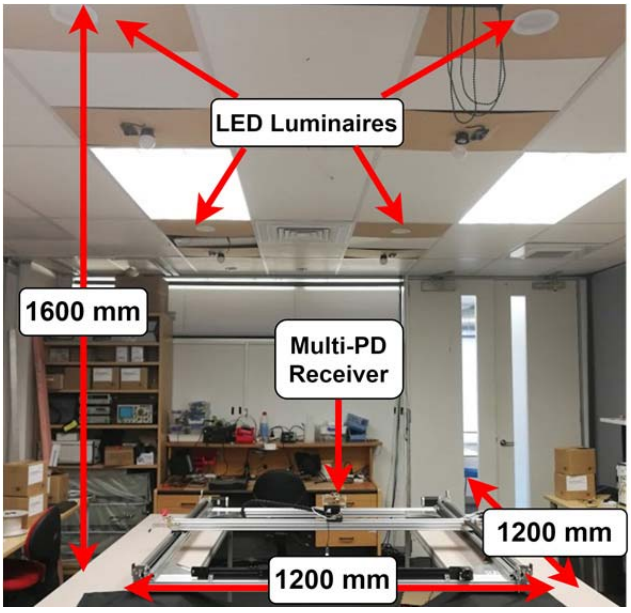

(b)

Fig. 3. Experimental setup. (a) Multiple-PD receiver mounted onto the CNC machine. (b) VLP Fingerprinting testbed.

III. Weighted k-Nearest Neighbors

Once the off-line database has been constructed, a matching algorithm can be used to estimate the position of the receiver during the online stage. The localization accuracy of a fingerprint-based system is affected by the matching algorithm used [17]. In this work, we implemented the WkNN algorithm as a regressor as it has been shown to be quite accurate for VLP systems [33]. The positioning accuracy of the WkNN algorithm was also found to be superior (please refer to Section IV for the comparative results) compared with that of an MLP that is a class of ANN.

The WkNN algorithm computes the distances of the neighbors and assigns weights to the distances such that the neighbor with a smaller distance has a greater weighting compared with the neighbor with a greater distance. Let the off-line location be denoted as (x_i, y_i), while the online location is denoted as $(x_j^{\text{live}}, y_j^{\text{live}})$.

The distance $d_{i,j}$ between (x_i, y_i) and $(x_j^{\text{live}}, y_j^{\text{live}})$ is computed using a distance metric with the Euclidean distance being the most common. The k-nearest neighbors are chosen such that they have the smallest distance and the largest weighting. The estimated position of the receiver $(\tilde{x}_j, \tilde{y}_j)$ is computed as the weighted average of the location of the k-nearest neighbors and is given by

$$\tilde{x}_j = \frac{\sum_{b=1}^{k} w_{j,b} \times x_b}{\sum_{b=1}^{k} w_{j,b}}, \quad \tilde{y}_j = \frac{\sum_{b=1}^{k} w_{j,b} \times y_b}{\sum_{b=1}^{k} w_{j,b}} \tag{1}$$

where (x_b, y_b) is the location of the bth neighbor from the k-nearest neighbors and the weight $w_{j,b}$ is the reciprocal of the distance $d_{j,i}$ [33]. The value of k needs to be chosen carefully. If a small k is used, it will not fit the data well, while a large k will lead to overfitting.

IV. Experimental Result and Discussion

One hundred sixty-nine equally spaced measurement locations were selected at 100-mm intervals within the 1200 × 1200 mm space. At each location, the RSS at each PD for each luminaire was measured resulting in 16 RSS recordings. Thirty-two sets of such RSS readings were taken at each location. Some of the locations are used to construct 32 sets of off-line databases corresponding to a 200 mm × 200 mm grid spacing, while the rest is used for the online phase and validation. All results presented in the subsequent sections are averaged over the data sets. A sparse fingerprint database corresponding to a 400 mm × 400 mm grid spacing is also constructed for comparison and data fabrication purposes(see

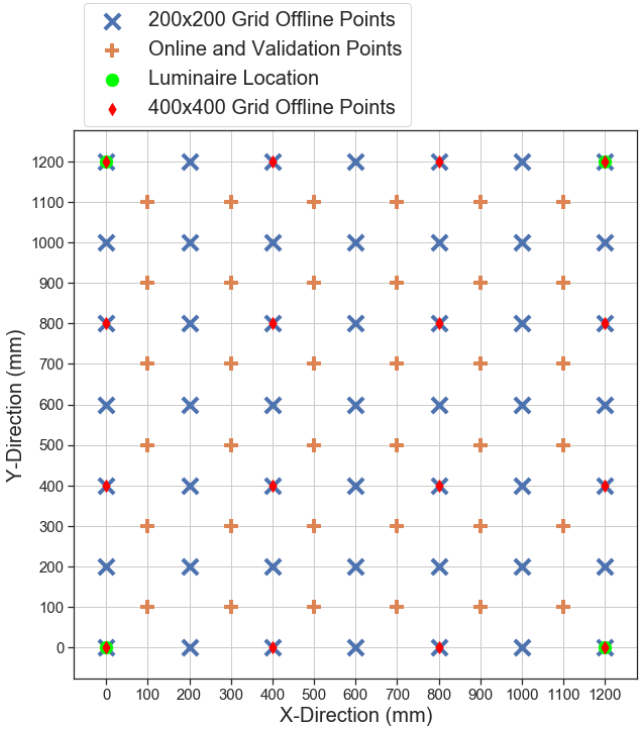

Fig. 4. Location of LED luminaires and test points used. Note that the off-line 400 × 400 locations are also used for fingerprint fabrication and the calibration of the HTC Vive.

Section V). Fig. 4 shows all these details. The receiver orientation is kept constant for all the experiments. The top PD has all four luminaires within its FOV throughout the experiments and provides the most reliable RSS feature and the smallest localization error. Therefore, it is used to emulate a single-PD system for comparison purposes. Two of the tilted PDs have three luminaires within their FOV for at least half the measurement locations, whereas the remainder PD has only two luminaires within its FOV throughout the experiment. Initial investigations show that the optimum number of neighbors, K, is either 3 or 4. While reporting the experimental results, one of these values for K was used, depending on whichever resulted in lower localization error. The denser 200 × 200 fingerprint provides significantly higher localization accuracy compared with the sparse 400 × 400 fingerprints with median errors of 3.78 and 25.48 mm, respectively. More details of these preliminary findings can be found in [36].

A. Effects of Number of PDs and Luminaires

Fig. 5 shows the cumulative distribution function (CDF) of the localization error of the multi-PD system for varying number of luminaires. Using the RSS from more luminaires improves the localization accuracy. The performance of the system when only the RSS from top PD is used is also provided. The RSS feature extracted from four PDs has more information compared with the RSS feature recovered with one PD (see Fig. 1 for an example). Therefore, a higher localization accuracy can be achieved using four PDs compared with using a single PD for the same number of luminaires. For the four-PD case, the localization accuracy degrades significantly only

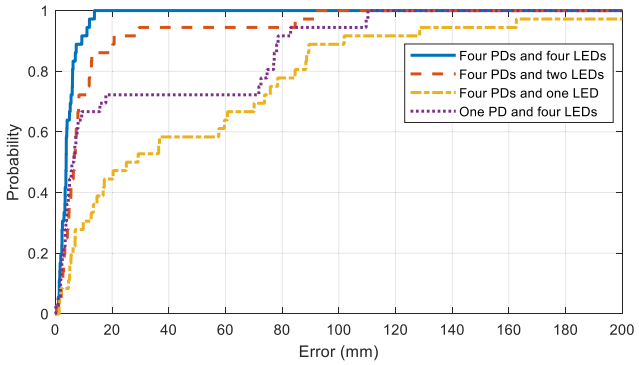

Fig. 5. Localization error for a four-PD array for a various number of luminaires. CDF of a single-PD system with four luminaires is shown for benchmarking. With four PDs, median and 90 percentile errors are 3.78 and 8.32 mm, respectively, with four luminaires, while, with two luminaires, median and 90 percentile errors are 6.63 and 20.45 mm. Median and 90 percentile errors for single PD are 6.17 and 78.31 mm, respectively.

for the one luminaire scenario. In contrast, the performance of the single-PD case degrades significantly when the number of luminaires is less than 3. It can also be observed that higher localization accuracy can be achieved when using the RSS at four PDs from two luminaires compared with using RSS at a single (top) PD from four luminaires.

B. Impact of Distance Metrics

As discussed in Section IV, the distance $d_{i,j}$ between (x_i, y_i) and $(x_j^{\text{live}}, y_j^{\text{live}})$ is computed, and the weight of the WkNN regressor is then estimated as the reciprocal of the distance. While the Euclidean distance metric is most commonly used, the literature [33] shows that the localization accuracy of a VLP using WkNN depends on the distance metrics utilized. Consequently, eight different distance metrics were explored and used to compute the weights for the WkNN algorithm. Table II shows the localization error for the various distance metrics using four PDs and four luminaires. It can be observed that the Euclidean distance is one of the better-performing metrics. However, the Manhattan and Matusita distances outperform the Euclidean distance for all scenarios. It is interesting to observe that the Lorentzian distance metric performs very accurately for 200 × 200 grid spacing but has low accuracy for the larger 400 × 400 grid spacing. The metric, due to its logarithmic nature, is more sensitive to smaller distances and less for larger distances. Therefore, it performs well when the fingerprint is dense (e.g., 200 × 200 database) with smaller distances between the RSS histograms of the live location and the potential neighbors. However, this advantage is nullified for sparse fingerprint (e.g., 400 × 400) with comparatively larger distances. In such a scenario, the Lorentzian distance metrics are also prone to misidentify the neighbors (e.g., 20% of the neighbors incorrectly identified compared with only 9% for Euclidean) resulting in large localization errors.

C. Neural Network-Based Localization

ANN-based VLP systems that have been proposed in the literature [34], [38]–[40] utilize feedforward neural networks

TABLE II

LOCALIZATION ERROR FOR VARIOUS DISTANCE METRIC USING FOUR PDS AND FOUR LUMINAIRES ($K = 4$ FOR 200×200 AND $K = 3$ FOR 400×400) WHERE $P_{n,j}^{\text{LIVE}}$ IS THE RSS AT ONLINE LOCATION (x_j, y_j) AND $P_{n,i}$ IS RSS AT OFF-LINE LOCATION (x_i, y_i). $N = 16$ (NUMBER OF RSS READING AT FOUR PD EACH FROM FOUR LUMINAIRES)

Distance Metric	Definition	Localization Error (mm)			
		200 x 200		400x400	
		Median	90 Perc.	Median	90 Perc.
Euclidean	$d_{j,i} = \sqrt{\sum_{n=1}^{N}(P_{n,j}^{live} - P_{n,i})^2}$	**3.78**	**8.33**	**25.48**	**93.07**
Manhattan	$d_{j,i} = \sum_{n=1}^{N}\lvert P_{n,j}^{live} - P_{n,i}\rvert^2$	**3.15**	**5.48**	**22.1**	**37.05**
Chebyshev	$d_{j,i} = \max_{n}\lvert P_{n,j}^{live} - P_{n,i}\rvert$	10.57	18.36	40.24	122.54
Squared Euclidean	$d_{j,i} = \sum_{n=1}^{N}(P_{n,j}^{live} - P_{n,i})^2$	7.53	15.81	62.4	77.33
Squared Chord	$d_{j,i} = \sum_{n=1}^{N}(\sqrt{P_{n,j}^{live}} - \sqrt{P_{n,i}})^2$	6.47	14.46	61.76	78.58
Matusita	$d_{j,i} = \sqrt{\sum_{n=1}^{N}(\sqrt{P_{n,j}^{live}} - \sqrt{P_{n,i}})^2}$	**3.42**	**7.53**	**24.25**	**31.47**
Canberra	$d_{j,i} = \sum_{n}^{N}\frac{\lvert P_{n,j}^{live} - P_{n,i}\rvert}{\lvert P_{n,j}^{live} + P_{n,i}\rvert}$	3.89	6.65	26.16	118.2
Lorentzian	$d_{j,i} = \log(1 + \lvert P_{n,j}^{live} - P_{n,i}\rvert)$	**1.15**	**3.4**	41.37	155.06

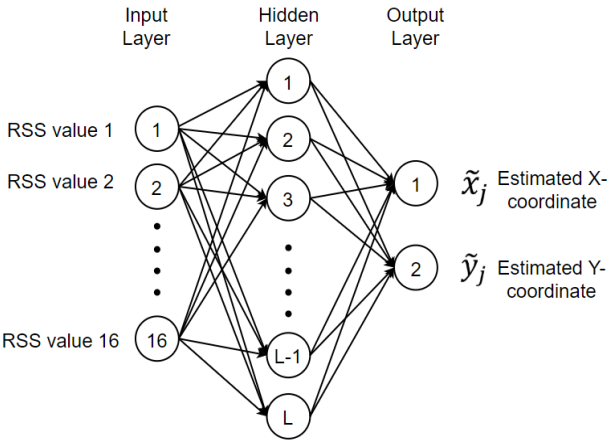

Fig. 6. Structure of the proposed MLP-based localization algorithm.

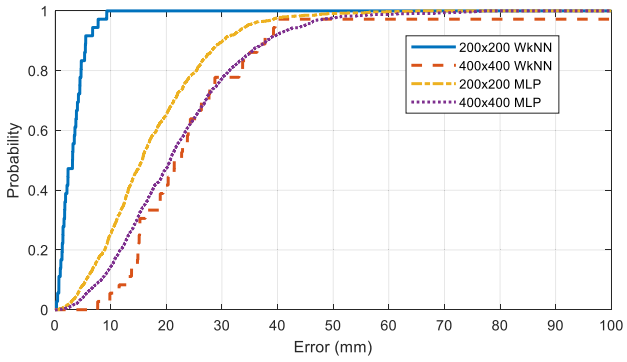

Fig. 7. Localization error for the WkNN and MLP algorithms for the dense (200×200) and sparse (400×400) fingerprint databases.

and backpropagation (BP) algorithms using one or two hidden layers. We developed a localization algorithm based on the MLP that is a class of feedforward ANN [41] and used it to benchmark the performance of WkNN.

The MLP is composed of an input layer, a hidden layer, and an output layer of which each layer consists of nodes that are fully connected to one another. The structure of the proposed MLP-based algorithm is shown in Fig. 6 and can be expressed by

$$N_{\text{out}} = \sum_{i=1}^{L} w_i \left(f\left(\sum_{j=1}^{16} w_j N_{\text{in}} + b_{0j} \right) \right) + b_{1i} \qquad (2)$$

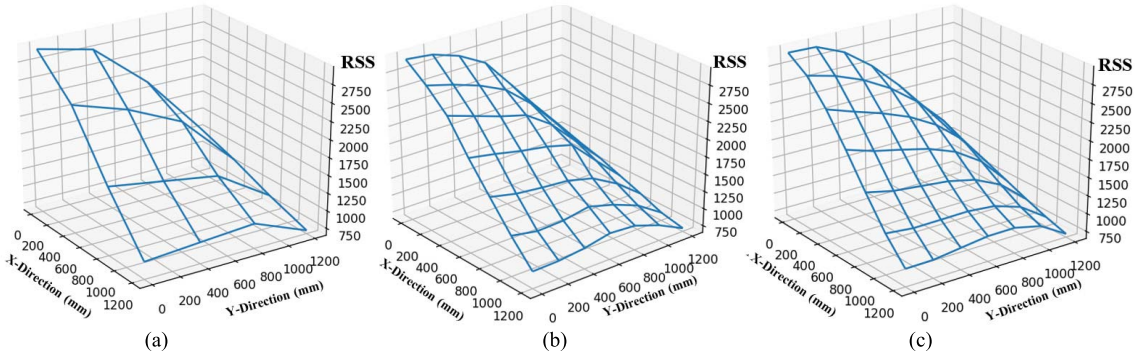

Fig. 8. Mesh grid showing the RSS at the top PD, PD0, and one luminaire for different grid spacing and databases. (a) Real 400 mm × 400 mm. (b) Real 200 mm × 200 mm. (c) Fabricated 200 mm × 200 mm.

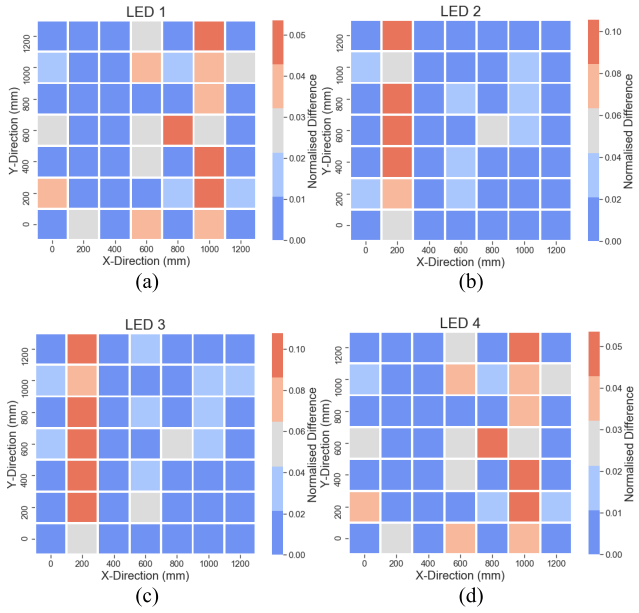

Fig. 9. Difference between the real and fabricated RSS for various luminaires at the top PD. (a) RSS difference at luminaire 1. (b) RSS difference at luminaire 2. (c) RSS difference at luminaire 3. (d) RSS difference at luminaire 4.

where f, w, b, and L are the activation function, weights, bias, and the number of nodes in the hidden layer, respectively. N_{in} is an input vector with a dimension of 16, while N_{out} is the output vector with dimension 2. The values were chosen based on the number of input value (16 RSS values from four luminaires and four PDs) and output value [estimated $(\tilde{x}_j, \tilde{y}_j)$]. The MLP was trained with the 32 sets of RSS measurement data taken at each test point. Increasing the number of hidden layers and the number of nodes in an MLP increases complexity and can lead to overfitting [39]. Therefore, one hidden layer was chosen for this work. To determine the optimal number of nodes for the hidden layer, the effects of the number of nodes on the localization error were verified. It was found that the optimal number of nodes was 10 and 19 for the 200 × 200 and 400 × 400 databases, respectively.

Fig. 7 shows the localization error for the two ML algorithms for the two different databases. The WkNN algorithm significantly outperforms the MLP for the 200 × 200 database but has similar performance to the MLP for the 400 × 400 database. When moving to a denser fingerprint, the accuracy improvement for the WkNN algorithm is greater than that of MLP. This is likely due to the regular arrangement of the additional datapoints being captured better by the WkNN algorithm as it uses a distance-based classification stage for neighbor identification leading to a strong relationship between density and accuracy. This increased density is not as directly incorporated into the MLP model as the additional datapoints must be used to update the networks' weights and biases during training. While increasing the number of measurements at each test point can potentially increase the performance of the MLP algorithm, it may not be feasible due to the cost of an off-line site survey in terms of labor and time and computational complexity.

V. Fingerprint Construction With Data Fabrication

The complexity and localization accuracy of a fingerprint-based system are affected by the size of the database. While fingerprint systems are easy to implement, for high localization accuracy, a dense, large database is needed making them time-consuming and labor-intensive. Data fabrication can be used to construct a dense fingerprint database from a sparse one. It has been shown to be quite effective for wireless-based localization [42] and visible light [33]-based localization. In this section, a simple and effective method of constructing a large fingerprint database with a small number of off-line measurements is presented. The proposed method uses a 2-D bivariate spline (B-spline) that is an interpolation technique of two variables [43]. The method is used to take the RSS values of a sparse 2-D grid and interpolate them. Through interpolation, RSS values at locations that are not directly on the grid can be fabricated, thus increasing the density of the grid.

Since a 1-D spline interpolation requires at least four points, a 2-D interpolation requires at least a 4 × 4 grid. Interpolation is only able to estimate values within the range of the data. Therefore, the vertices of the desired grid must be included. The points should be equally and widely distributed across the experimental setup. For this experiment, the 16 points from the

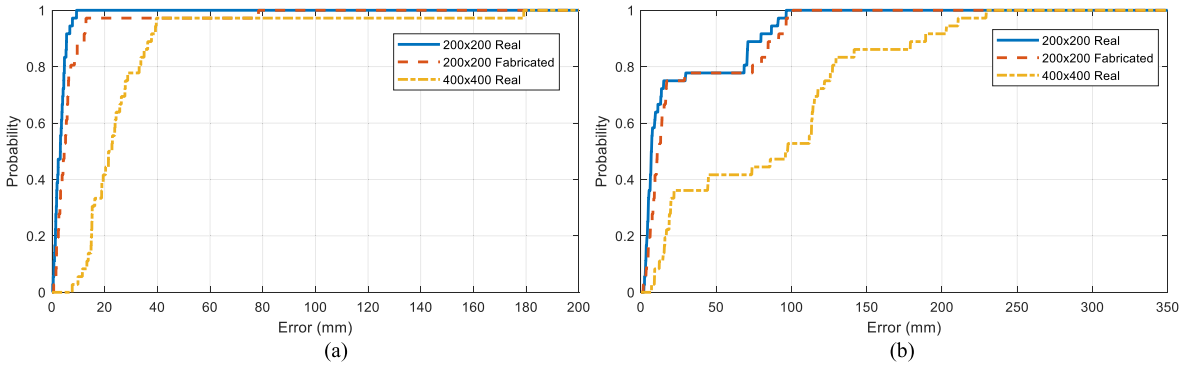

Fig. 10. Localization error using the Manhattan distance metric for two different scenarios. (a) Four PDs and four luminaires. (b) Four PDs and two luminaires. "200 × 200 Real" and "400 × 400 Real" fingerprint are constructed from actual RSS measured at the corresponding off-line locations shown in Fig. 4. "200 × 200 Fabricated" dense fingerprint constructed to emulate the "200 × 200 Real" fingerprint by interpolating the "400 × 400 Real" fingerprint.

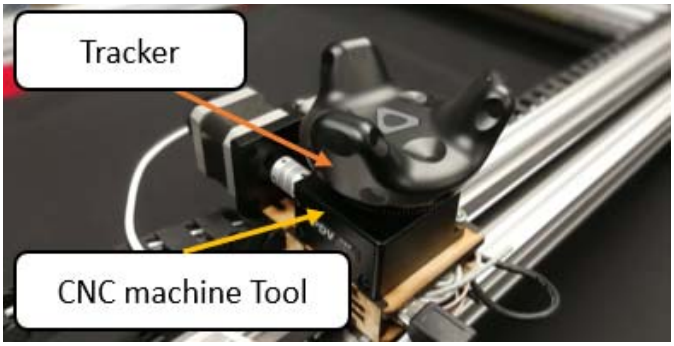

Fig. 11. HTC Vive's Tracker mounted on the tool of the CNC machine.

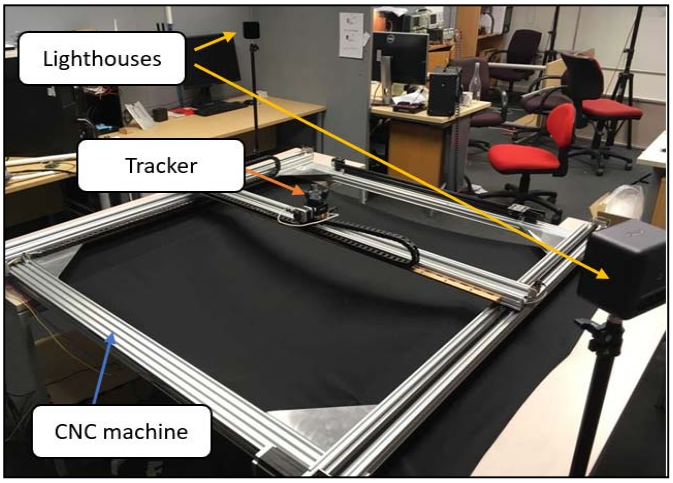

Fig. 12. Vive experimental setup with two lighthouses and the tracker on the CNC machine.

400 × 400 grid off-line points shown in Fig. 4 were chosen. These points are then used to fabricate the 36 points from the 200 × 200 grid off-line points shown in Fig. 4.

Fig. 8 shows the mesh grid RSS for different scenarios. Fig. 9 illustrates the difference in RSS between the fabricated data and the real data for the horizontal PD for all four luminaires. As we can observe, the fabricated RSS emulates the real data reasonably accurately with a maximum difference of approximately 10%. Therefore, it is expected that data fabrication will not cause significant degradation in localization accuracy. This is supported in Fig. 10 that shows the CDF of localization error using the Manhattan distance, the best performing distance, for two scenarios. It can be observed that the localization error with the 200 × 200 fabricated database is slightly higher compared with that achieved from the measured 200 × 200 real database. However, the localization performance with the fabricated data is much better than that achieved with the sparse 400 × 400 real database. Therefore, data fabrication allows the utilization of a smaller fingerprint database and, thereby, reduces the cost of labor and time of off-line measurement. This makes the proposed fingerprint-based approach less data-driven. A new fingerprint can be easily constructed from a small number of measurements to respond to any change in the environment or the hardware. Recent advances in RSS-based VLP [44] can also be explored to make the approach more robust. Table III shows the localization error statistics for both Manhattan and Euclidean distances for the three different scenarios. It can be seen that the Manhattan distance outperforms the Euclidean distance for both real and fabricated data.

VI. Benchmarking VLP Against HTC Vive

The localization performance of the developed multi-PD VLP system was benchmarked against a commercial solution, the HTC Vive, which is a reliable motion capture technology used for consumer virtual reality (VR) application. A Vive tracker, an accessory with tracking functionality, was selected as the target. Two HTC Vive base stations, also known as lighthouses, transmit synchronized light sweeps for localizing the tracker using the AoA technique [45]. While the system can operate with one lighthouse, two synchronized lighthouses achieve better accuracy [46]. It should be noted that the tracker also fuses data from its IMU. The tracker is mounted on the CNC's tool (see Fig. 11) for moving it within the 1200 × 1200 mm test area. Fig. 12 shows the setup of the experiment. The positional data are transferred from the Bluetooth equipped tracker to a PC connected with a Vive wireless dongle.

TABLE III
LOCALIZATION ERROR FOR VARIOUS DISTANCE METRICS USING FOUR PDS AND FOUR LUMINAIRES (LED = 4)

Distance Metric	Localization Error (mm)					
	Real 200 x 200		Real 400 x 400		Fabricated 200 x 200	
	Median	90 Perc.	Median	90 Perc.	Median	90 Perc.
Euclidean	3.78	8.33	25.48	93.07	4.74	12.12
Manhattan	3.15	5.48	22.1	37.05	4.62	10.87

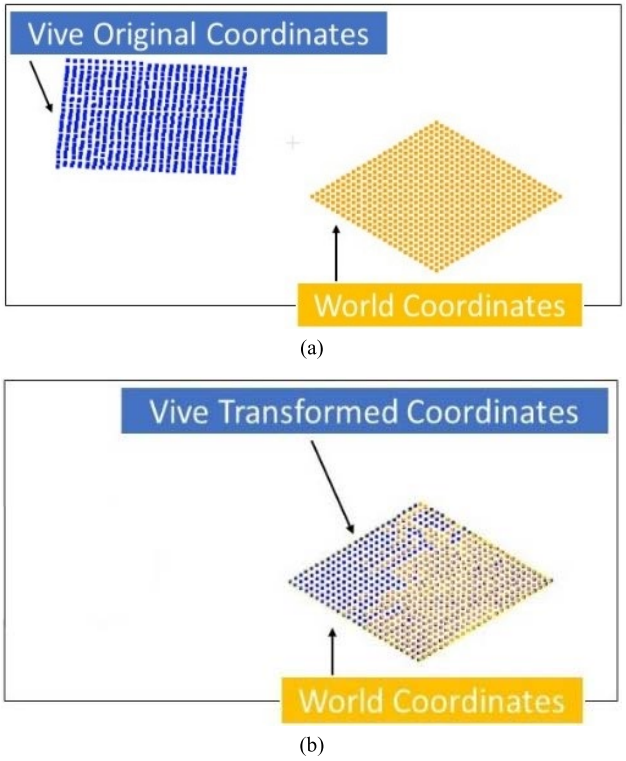

Fig. 13. Illustration of Vive coordinates and world coordinates for two different scenarios. (a) Before point mapping. (b) After point mapping.

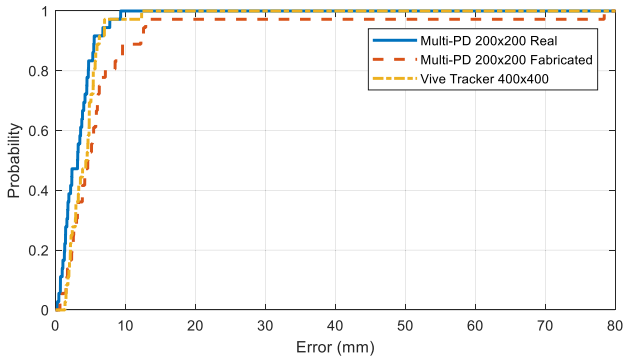

Fig. 14. Localization error for the developed multi-PD system using four PDs, four luminaires, and Manhattan distance and the HTC Vive.

The positional values given by the HTC Vive are based on the system's local coordinate system [refer to Fig. 13(a)], where the origin is the center point of the Vive's lighthouse. Therefore, point mapping or coordinate transformation is needed to be applied to convert the coordinates into our defined world coordinate [see Fig. 13(b)]. The tracker is placed at 16 known reference points (the same number of points used for the RSS data fabrication) to configure the coordinate transformation. These reference points are located at the 400 × 400 grid off-line points shown in Fig. 4. Due to noises and outliers in the data set, it is not ideal to determine the spatial transformation matrices using only trigonometry rules. We applied iterative closest point (ICP), a point set registration technique that determines an unknown spatial transformation to align two sets of points [47], and the 16 reference points in our case. Although this technique is effective [48], it requires the two sets to be relatively close to make sure that the correct points are matched to its corresponding reference points reliably. Therefore, a rough alignment is required preceding ICP, which is achieved based on axis translation (to align the local coordinate's origin to the reference origin) and subsequent rotation through the application of Euler's rotation theorem [49]. The ICP is performed with the 16 reference points to compute the calibration transformation matrix.

The localization error of the developed multi-PD system and the HTC Vive are compared in Fig. 14 by plotting the CDF of the localization error. It can be seen that the performance of the developed system is comparable to the Vive with slightly better localization accuracy with actual data and marginally worse with the fabricated data. However, it should be noted that, in contrast to the Vive that utilizes IMU data and continuous tracking, the developed VLP is currently set up as a "single-shot" [50] system. Consequently, further improvement can potentially be achieved by fusing the onboard IMU to track transitions between test points.

VII. CONCLUSION

This article presents a visible light-based positioning method using four PDs. The multiple-PD-based system has higher localization accuracy and can function with less number of visible luminaires compared with a single-PD-based system. The localization error can be further reduced by selecting either the Manhattan or Matusita distance metrics for the WkNN algorithm. Data fabrication through simple 2-D interpolation is shown to be an effective way of reducing the cost of time and labor of an off-line site survey. A median error of 4.74 mm can be achieved for four luminaires, while a median error of 9.87 mm can be achieved with two luminaires. Among the two ML algorithms investigated, WkNN was found to be more accurate than MLP for our experimental setup. The developed VLP system was benchmarked against an HTC Vive. The VLP's performance was comparable to that of the common commercial solution while producing similar error

statistics with a lower number of small errors with a slightly greater number of larger errors.

The developed multi-PD receiver could potentially perform 3-D positioning via a fingerprint- or model-based method. For the fingerprint approach, it is difficult to acquire 3-D off-line database. However, it may be possible to utilize 3-D interpolation- or ML-based regression to fabricate a dense 3-D fingerprint from a set of RSS data collected at a few different receiver heights. Model-based methods might be preferred because they allow for changing receiver orientation that is an issue with fingerprint techniques. Using just the signals from multiple luminaires and PDs, it is possible to determine the receiver's 3-D position and orientation [51]. An IMU that is already available onboard the receiver (see Fig. 2) can provide the receiver's normal vector [9] and would likely improve positioning accuracy although this has not yet been explored in the literature. The major drawback of model-based 3-D positioning with multiple PDs is that the resulting expressions are complex and nonconvex and need to be solved using iterative approaches not suited for embedded applications. It should be noted that while 3-D positioning has many applications, the addition of an extra dimension comes at the cost of decreased accuracy [25], [26], and for an application not requiring it, this tradeoff may not have enough benefit.

Throughout the experiments, the orientation of the VLP receiver was kept unchanged. While this is a realistic assumption for robotic applications (a simple gimbal can achieve this), the impact of orientation change needs to be explored. The orientation of the receiver might not have been optimal orientation as the luminaires were not within the FOV of the all PDs for all locations. It may be possible to determine the optimum orientation for a particular setup. In a real-world environment, online locations would not always be on a regular grid. Hence, random online points can be used to test the performance in such a scenario. Future work could also include implementing model-based localization using the multi-PD receiver board. A comparative benchmarking against existing VLP solutions has also been left for future investigation. Data fabrication was achieved through the 2-D interpolation technique. Investigation of other interpolation and model-based data regeneration techniques have been left for future research. Localization algorithms based on other ML techniques can also be explored. Future works could include using arbitrary test locations rather than evenly spaced points as that practice has been reported to improve the localization performance of NN [40]. The VLP system needs to be tested for a larger experimental setup. The low localization error of the developed VLP system also necessitates an extremely accurate ground-truth recording procedure. These restrictions had constrained the size of the experimental setup. The localization algorithms were trained with a relatively small number of data sets. They need to be trained and tested with more extensive data sets and, thus, require a large number of RSS recordings at each test location. Therefore, the development of an accurate and automated ground-truth recording system can be an interesting research topic for the future.

REFERENCES

[1] F. Van Diggelen and P. Enge, "The world's first GPS MOOC and worldwide laboratory using smartphones," in *Proc. 28th Int. Tech. Meeting Satell. Division Inst. Navigat. (ION GNSS)*, 2015, pp. 361–369.

[2] INFSOFT. *Indoor Navigation & Services in Airports*. Accessed: Oct. 10, 2019. [Online]. Available: https://www.infsoft.com/industries/airports/features

[3] V. Bianchi, P. Ciampolini, and I. De Munari, "RSSI-based indoor localization and identification for ZigBee wireless sensor networks in smart homes," *IEEE Trans. Instrum. Meas.*, vol. 68, no. 2, pp. 566–575, Feb. 2019, doi: 10.1109/TIM.2018.2851675.

[4] B. Xie *et al.*, "LIPS: A light intensity-based positioning system for indoor environments," *ACM Trans. Sensor Netw.*, vol. 12, no. 4, pp. 1–27, Nov. 2016, doi: 10.1145/2953880.

[5] R. Carotenuto, M. Merenda, D. Iero, and F. G. D. Corte, "An indoor ultrasonic system for autonomous 3-D positioning," *IEEE Trans. Instrum. Meas.*, vol. 68, no. 7, pp. 2507–2518, Jul. 2019, doi: 10.1109/TIM.2018.2866358.

[6] J. Fang *et al.*, "High-speed indoor navigation system based on visible light and mobile phone," *IEEE Photon. J.*, vol. 9, no. 2, pp. 1–11, Apr. 2017, doi: 10.1109/JPHOT.2017.2687947.

[7] J. Rabadan, V. Guerra, R. Rodríguez, J. Rufo, M. Luna-Rivera, and R. Perez-Jimenez, "Hybrid visible light and ultrasound-based sensor for distance estimation," *Sensors*, vol. 17, no. 2, p. 330, Feb. 2017, doi: 10.3390/s17020330.

[8] L. Cheng, W. Viriyasitavat, M. Boban, and H.-M. Tsai, "Comparison of radio frequency and visible light propagation channels for vehicular communications," *IEEE Access*, vol. 6, pp. 2634–2644, 2018, doi: 10.1109/ACCESS.2017.2784620.

[9] M. Yasir, S.-W. Ho, and B. N. Vellambi, "Indoor position tracking using multiple optical receivers," *J. Lightw. Technol.*, vol. 34, no. 4, pp. 1166–1176, Feb. 15, 2016, doi: 10.1109/JLT.2015.2507182.

[10] T. Akiyama, M. Sugimoto, and H. Hashizume, "Time-of-arrival-based smartphone localization using visible light communication," in *Proc. Int. Conf. Indoor Positioning Indoor Navigat. (IPIN)*, Sep. 2017, pp. 1–7, doi: 10.1109/IPIN.2017.8115904.

[11] A. Naz, N. U. Hassan, M. A. Pasha, H. Asif, T. M. Jadoon, and C. Yuen, "Single LED ceiling lamp based indoor positioning system," in *Proc. IEEE 4th World Forum Internet Things (WF-IoT)*, Feb. 2018, pp. 682–687, doi: 10.1109/WF-IoT.2018.8355186.

[12] A. Arafa, X. Jin, and R. Klukas, "Wireless indoor optical positioning with a differential photosensor," *IEEE Photon. Technol. Lett.*, vol. 24, no. 12, pp. 1027–1029, Jun. 15, 2012, doi: 10.1109/LPT.2012.2194140.

[13] S. Zhang, W.-D. Zhong, P. Du, and C. Chen, "Experimental demonstration of indoor sub-decimeter accuracy VLP system using differential PDOA," *IEEE Photon. Technol. Lett.*, vol. 30, no. 19, pp. 1703–1706, Oct. 1, 2018, doi: 10.1109/LPT.2018.2866402.

[14] H. Steendam, T. Q. Wang, and J. Armstrong, "Cramér-Rao bound for AOA-based VLP with an aperture-based receiver," in *Proc. IEEE Int. Conf. Commun. (ICC)*, May 2017, pp. 1–6, doi: 10.1109/ICC.2017.7996691.

[15] J. H. Y. Nah, R. Parthiban, and M. H. Jaward, "Visible light communications localization using TDOA-based coherent heterodyne detection," in *Proc. IEEE 4th Int. Conf. Photon. (ICP)*, Oct. 2013, pp. 247–249, doi: 10.1109/ICP.2013.6687128.

[16] Z. Yang, Z. Wang, J. Zhang, C. Huang, and Q. Zhang, "Wearables can afford: Light-weight indoor positioning with visible light," presented at the 13th Annu. Int. Conf. Mobile Syst., Appl., Services, Florence, Italy, 2015.

[17] Y. Zhuang *et al.*, "A survey of positioning systems using visible LED lights," *IEEE Commun. Surveys Tuts.*, vol. 20, no. 3, pp. 1963–1988, 3rd Quart., 2018, doi: 10.1109/COMST.2018.2806558.

[18] Y. C. See, N. M. Noor, and C. T. Y. M, "Investigation of indoor positioning system using visible light communication," in *Proc. IEEE Region Conf. (TENCON)*, Nov. 2016, pp. 186–189, doi: 10.1109/TENCON.2016.7847986.

[19] W. Liu, X. Fu, Z. Deng, L. Xu, and J. Jiao, "Smallest enclosing circle-based fingerprint clustering and modified-WKNN matching algorithm for indoor positioning," in *Proc. Int. Conf. Indoor Positioning Indoor Navigat. (IPIN)*, Oct. 2016, pp. 1–6, doi: 10.1109/IPIN.2016.7743694.

[20] S.-H. Yang, E.-M. Jung, and S.-K. Han, "Indoor location estimation based on LED visible light communication using multiple optical receivers," *IEEE Commun. Lett.*, vol. 17, no. 9, pp. 1834–1837, Sep. 2013, doi: 10.1109/LCOMM.2013.070913.131120.

[21] S.-H. Yang and S.-K. Han, "VLC based indoor positioning using single-Tx and rotatable single-Rx," in *Proc. 12th Int. Conf. Opt. Internet (COIN)*, Aug. 2014, pp. 1–2, doi: 10.1109/COIN.2014.6950557.

[22] W. Xu, J. Wang, H. Shen, H. Zhang, and X. You, "Indoor positioning for multiphotodiode device using visible-light communications," *IEEE Photon. J.*, vol. 8, no. 1, pp. 1–11, Feb. 2016, doi: 10.1109/JPHOT.2015.2513198.

[23] X. Yu, J. Wang, and H. Lu, "Single LED-based indoor positioning system using multiple photodetectors," *IEEE Photon. J.*, vol. 10, no. 6, pp. 1–8, Dec. 2018, doi: 10.1109/JPHOT.2018.2848947.

[24] E.-M. Jeong, S.-K. Han, S.-H. Yang, and H.-S. Kim, "Tilted receiver angle error compensated indoor positioning system based on visible light communication," *Electron. Lett.*, vol. 49, no. 14, pp. 890–892, Jul. 2013, doi: 10.1049/el.2013.1368.

[25] S. H. Yang, H. S. Kim, Y. H. Son, and S. K. Han, "Three-dimensional visible light indoor localization using AOA and RSS with multiple optical receivers," *J. Lightw. Technol.*, vol. 32, no. 14, pp. 2480–2485, Jul. 15, 2014.

[26] X. Yu, J. Wang, and H. Lu, "Indoor positioning system based on single LED using symmetrical optical receiver," in *Proc. Asia Commun. Photon. Conf. (ACP)*, Oct. 2018, pp. 1–3, doi: 10.1109/ACP.2018.8596193.

[27] L. Wang and C. Guo, "Indoor visible light localization algorithm with multi-directional PD array," in *Proc. IEEE Globecom Workshops (GC Wkshps)*, Dec. 2017, pp. 1–6, doi: 10.1109/GLOCOMW.2017.8269149.

[28] M. Yasir, S.-W. Ho, and B. N. Vellambi, "Indoor positioning system using visible light and accelerometer," *J. Lightw. Technol.*, vol. 32, no. 19, pp. 3306–3316, Oct. 1, 2014, doi: 10.1109/JLT.2014.2344772.

[29] B. Xie, S. Gong, and G. Tan, "LiPro: Light-based indoor positioning with rotating handheld devices," *Wireless Netw.*, vol. 24, no. 1, pp. 49–59, Jan. 2018, doi: 10.1007/s11276-016-1312-1.

[30] F. Zafari, A. Gkelias, and K. Leung, "A survey of indoor localization systems and technologies," 2017, *arXiv:1709.01015*. [Online]. Available: http://arxiv.org/abs/1709.01015

[31] W. H. Ali, A. A. Kareem, and M. Jasim, "Survey on wireless indoor positioning systems," *Cihan Univ.-Erbil Sci. J.*, vol. 3, no. 2, pp. 42–47, Aug. 2019, doi: 10.24086/cuesj.v3n2y2019.pp42-47.

[32] J. Yoo, K. H. Johansson, and H. J. Kim, "Indoor localization without a prior map by trajectory learning from crowdsourced measurements," *IEEE Trans. Instrum. Meas.*, vol. 66, no. 11, pp. 2825–2835, Nov. 2017, doi: 10.1109/TIM.2017.2729438.

[33] F. Alam, M. T. Chew, T. Wenge, and G. S. Gupta, "An accurate visible light positioning system using regenerated fingerprint database based on calibrated propagation model," *IEEE Trans. Instrum. Meas.*, vol. 68, no. 8, pp. 2714–2723, Aug. 2019, doi: 10.1109/TIM.2018.2870263.

[34] C. Lin *et al.*, "An indoor visible light positioning system using artificial neural network," in *Proc. Asia Commun. Photon. Conf. (ACP)*, Oct. 2018, pp. 1–3, doi: 10.1109/ACP.2018.8596227.

[35] S. Alraih, A. Alhammadi, I. Shayea, and A. M. Al-Samman, "Improving accuracy in indoor localization system using fingerprinting technique," in *Proc. Int. Conf. Inf. Commun. Technol. Converg. (ICTC)*, Oct. 2017, pp. 274–277, doi: 10.1109/ICTC.2017.8190985.

[36] A. Hasan, T. Glass, F. Alam, and M. Legg, "Fingerprint-based visible light positioning using multiple photodiode receiver," presented at the IEEE Sensors Appl. Symp. (SAS), Kuala Lumpur, Malaysia, Mar. 2020.

[37] F. Alam, B. Parr, and S. Mander, "Visible light positioning based on calibrated propagation model," *IEEE Sens. Lett.*, vol. 3, no. 2, pp. 1–4, Feb. 2019, doi: 10.1109/LSENS.2018.2889270.

[38] I. Alonso-González, D. Sánchez-Rodríguez, C. Ley-Bosch, and M. Quintana-Suárez, "Discrete indoor three-dimensional localization system based on neural networks using visible light communication," *Sensors*, vol. 18, no. 4, p. 1040, Mar. 2018, doi: 10.3390/s18041040.

[39] H. Zhang *et al.*, "High-precision indoor visible light positioning using modified momentum back propagation neural network with sparse training point," *Sensors*, vol. 19, no. 10, p. 2324, May 2019, doi: 10.3390/s19102324.

[40] J. He *et al.*, "Demonstration of high precision 3D indoor positioning system based on two-layer ANN machine learning technique," in *Proc. Opt. Fiber Commun. Conf. (OFC)*, Mar. 2019, pp. 1–3.

[41] H. Ramchoun, M. Amine, M. A. J. Idrissi, Y. Ghanou, and M. Ettaouil, "Multilayer perceptron: Architecture optimization and training," *Int. J. Interact. Multimedia Artif. Intell.*, vol. 4, pp. 26–30, Jan. 2016, doi: 10.9781/ijimai.2016.415.

[42] J. Racko, J. Machaj, and P. Brida, "Wi-Fi fingerprint radio map creation by using interpolation," *Procedia Eng.*, vol. 192, pp. 753–758, Jan. 2017.

[43] Y. Mehari, "Easy way to find multivariate interpolation," *Int. J. Emerg. Trends Sci. Technol.*, vol. 4, no. 5, pp. 5189–5193, May 2017, doi: 10.18535/ijetst/v4i5.11.

[44] N. Huang, C. Gong, J. Luo, and Z. Xu, "Design and demonstration of robust visible light positioning based on received signal strength," *J. Lightw. Technol.*, early access, Jun. 11, 2020, doi: 10.1109/JLT.2020.3001761.

[45] M. Borges, A. Symington, B. Coltin, T. Smith, and R. Ventura, "HTC vive: Analysis and accuracy improvement," in *Proc. IEEE/RSJ Int. Conf. Intell. Robots Syst. (IROS)*, Oct. 2018, pp. 2610–2615.

[46] W. Jansen, D. Laurijssen, W. Daems, and J. Steckel, "Automatic calibration of a six-degrees-of-freedom pose estimation system," *IEEE Sensors J.*, vol. 19, no. 19, pp. 8824–8831, Oct. 2019.

[47] A. Myronenko and X. Song, "Point set registration: Coherent point drift," *IEEE Trans. Pattern Anal. Mach. Intell.*, vol. 32, no. 12, pp. 2262–2275, Dec. 2010, doi: 10.1109/TPAMI.2010.46.

[48] R. S. J. Estépar, A. Brun, and C.-F. Westin, "Robust generalized total least squares iterative closest point registration," in *Medical Image Computing and Computer-Assisted Intervention*, C. Barillot, D. R. Haynor, and P. Hellier, Eds. Berlin, Germany: Springer, 2004, pp. 234–241.

[49] J. Diebel, "Representing attitude: Euler angles, unit quaternions, and rotation vectors," *Matrix*, vol. 58, pp. 1–35, Jan. 2006.

[50] A. Popleteev, "Wi-Fi butterfly effect in indoor localization: The impact of imprecise ground truth and small-scale fading," in *Proc. 14th Workshop Positioning, Navigat. Commun. (WPNC)*, Oct. 2017, pp. 1–5.

[51] S. Shen, S. Li, and H. Steendam, "Simultaneous position and orientation estimation for visible light systems with multiple LEDs and multiple PDs," *IEEE J. Sel. Areas Commun.*, vol. 38, no. 8, pp. 1866–1879, Aug. 2020, doi: 10.1109/JSAC.2020.3000805.

Adli Hasan Abu Bakar received the B.E. degree (Hons.) in electronic and computer engineering from Massey University, Auckland, New Zealand, in 2020, where he is currently pursuing the Ph.D. degree.

His research interests include wood acoustics, machine learning, and visible light positioning.

Tyrel Glass received the B.E. degree (Hons.) in electronic and computer engineering from Massey University, Auckland, New Zealand, in 2019, where he is currently pursuing the Ph.D. degree.

His research interests include visible light positioning, machine learning, big data, and the Internet of Things.

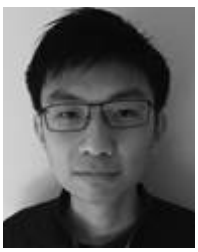

Hing Yan Tee received the B.E. degree (Hons.) in mechatronics engineering from Massey University, Albany, New Zealand, in 2020.

His research interests include robotics, machine learning, and the Internet of Things (IoT).

Fakhrul Alam (Senior Member, IEEE) received the B.Sc. degree (Hons.) in electrical and electronic engineering from the Bangladesh University of Engineering and Technology (BUET), Dhaka, Bangladesh, in 1996, and M.S. and Ph.D. degrees in electrical engineering from Virginia Tech, Blacksburg, VA, USA, in 1999 and 2002, respectively.

He is currently an Associate Professor with the Department of Mechanical and Electrical Engineering, School of Food & Advanced Technology, Massey University, Auckland, New Zealand. His research interests include indoor localization, 5G and visible light communication, the Internet of Things (IoT), and wireless sensor networks.

Dr. Alam is also a member of the IEEE I&M Society and the Institution of Engineering and Technology (IET).

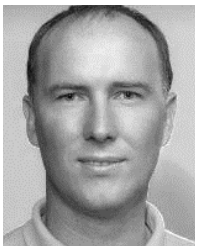

Mathew Legg (Member, IEEE) received the B.Sc., M.Sc., and Ph.D. degrees in physics from The University of Auckland, Auckland, New Zealand, in 2003, 2007, and 2012, respectively.

He is currently a Senior Lecturer with the Department of Mechanical and Electrical Engineering, School of Food & Advanced Technology, Massey University, Auckland. His research relates to the development of acoustic/ultrasonic measurement systems and techniques for acoustic imaging, nondestructive testing, and remote sensing.